Journal of Complex Flow, Vol. 4 No. 2 (2022) p. 17-25

FAZ Publishing

JCF

Journal of Complex Flow

Journal homepage: www.fazpublishing.com/jcf

e-ISSN : 2672-7374

Analysis of Flow Characteristics at the Stenotic Femoropliteal Artery

Muhd Aiman Zuhdi Zulkifli[1], Ishkrizat Taib[1,*]

[1] Faculty of Mechanical and Manufacturing Engineering,
Universiti Tun Hussein Onn Malaysia, Batu Pahat, 86400, MALAYSIA

*Corresponding Author

Received 2 June 2022;
Accepted 12 August 2022;
Available online 1 Sept 2022

Abstract: Femoropopliteal arterial disease is a narrowing of the blood vessel in the lower limp which might be clogged if not immediately treated. The blood flow characteristic at the stenotic region represents the flow recirculation which is prone to the growth of thrombosis. This phenomenon occurred due to the influence of hemodynamic factors such as low wall shear stress (WSSlow), normal WSS, and wall shear stress gradient (WSSG). The formation of thrombosis become severe with the growth of the stenotic region. Thus, this study aims to determine the flow characteristic due to the effect of the hemodynamic differences for different sizes of stenosis at the femoropopliteal artery. Four different geometrical models of the femoropopliteal artery with different sizes of stenosis are modelled. The computational fluid dynamic (CFD) method with the steady-state conditions was implemented in the study. Three different pulsating waveforms were also imposed: peak systolic, end-diastolic, and mid-diastolic. The result shows that the pressure drops abruptly in the stenotic region of Model D as compared to others. Furthermore, the velocity has also seen significant increases when the pressure drop. From the observation, the peak systolic time shows the lowest WSSlow whilst the end-diastolic shows the highest of WSSlow for all models. However, Model A shows the highest WSSlow percentages as compared to others which re-present the highest growth of atherosclerosis approximately 95.8 %. In a summary, the prediction of thrombosis formation is the highest for Model B, approximately 13.13%.

Keywords: Stenosis, atherosclerosis, thrombosis

1. Introduction

Arteriosclerosis is a common consequence of a variety of arterial diseases. The presence of protruding atherosclerotic plaques in the lumen narrows arteries, resulting in stenosis. When arteries get blocked, it causes increase resistance and, as a result, blood flow to the specific vascular bed serviced by the artery is reduced. Peripheral arterial disease (PAD) is a chronic arterial occlusive disorder of the lower limbs caused by atherosclerosis. PAD is defined as a weakness during walking that is relieved by rest, intermittent claudication, or pain. It happen when a plaque sets up around the arterial that provides oxygen in the blood to the legs, stomach, arms, and head. The accumulation of plaque and fat stiffening is known as a thrombus in the femoropopliteal artery causes peripheral arterial disease such as thrombosis. The blood flow via the artery will be disrupted as a result of this disease. The femoropopliteal artery thrombosis causes claudication, which is cramping pain in the leg muscle caused by the blockage in the femoropopliteal artery [1]

The presence of stenosis cause major circulation problems [2]. The presence of plaque causes stenosis, which is when the artery becomes unnaturally narrow. Stenosis arteries are a narrowing or constriction of the inner surface (lumen) of arteries. It plays a significant role in the development of well-known severe disorders such as cardiovascular disease and atherosclerosis [3]. Stenosis will cause a significant pressure drop, plaque rupture, increased wall shear stress (WSS), and affect blood flow [4]. Different sizes of stenosis have different effects on the hemodynamic parameters of the blood. The blood flow is disrupted once stenosis develops, and hemodynamic parameters play a significant role as the stenosis grows [5]. Blood is Newtonian fluid [6] and Newtonian fluid is described as the flow behaviour of fluids with a simple linear relation between shear stress (Pa) and shear rate (1/s). No matter how much shear is applied for a constant temperature, the viscosity of a Newtonian fluid remains constant [7]. Thus, liquid flow is typically incompressible [8].

**Corresponding author: iszat@uthm.edu.my*

Numerical computational modelling such as computational fluid dynamics or CFD is used to gain specifics about the flow field such as pressure profile, shear stresses, flow streamlines, and velocity [8]. CFD is a useful tool in addition to fluid mechanics experiments or observations because it provides extra data and allows for quick simulation of the effects of changes in geometry or boundary conditions. Most hemodynamic research has relied on computational fluid dynamics (CFD) approaches to fully understand several hemodynamic characteristics by treating blood as a single-phase Newtonian fluid [9]. Shear stress is caused by fluid flow across a surface and is directly proportional to the velocity of the fluid surrounding it. CFD techniques were the only means of estimating shear stress due to the lack of sensors [10]. Research indicates that wall shear stress (WSS) plays a critical role in the localization of atherosclerosis. Fluid does not flow at the same speed throughout a straight vessel in a non-pulsatile flow. Fluid flow is therefore fastest in the centre and slowest near the wall. The fluid velocities follow a parabolic pattern known as "laminar flow" [11].

The acceptable range of wall shear stress is 0.5 N/m^2. to 2 N/m^2 according to clinical studies. If the shear stress value is greater than or less than the range, it causes atherosclerosis. [12]. However, study from [13] stated that atherosclerosis is predicted to develop for the WSSlow to be less than 4 dyne/cm^2 and thrombosis may occur when WSS is greater than 70 dyne/cm^2.

In summary, four models of femoropopliteal artery with different size of stenosis were modelled and the computational fluid domain was used to simulate the models. Then hemodynamic parameters such as velocity distribution, pressure, wall shear stress, and low wall shear stress are analyses to study the flow characteristic for different sizes of stenosis at the femoropopliteal artery and predict the growth of thrombosis for different stenosis sizes.

2. Materials and Methods

2.1 The simplified model of femoropopliteal artery

The simplified model of Femoropopliteal artery (FPA) was developed using SOLIDWORK CAD software 2021 as illustrated in Figure 1. The simplification of this model was made to describe the hemodynamic effect on different sizes of stenosis. The simplified FPA model was modelled with 4 different sizes of stenosis as shown in Figure 2. The simplified FPA has a length (L) of 39 mm and a diameter (D) of 3.5 mm.

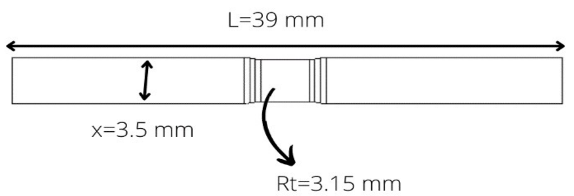

Fig. 1 - The simplified of FPA model

Type of simplified model	Simplified Model
Model A	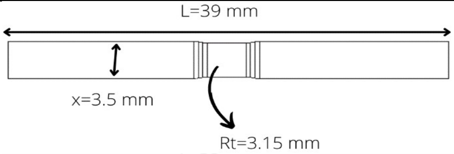
Model B	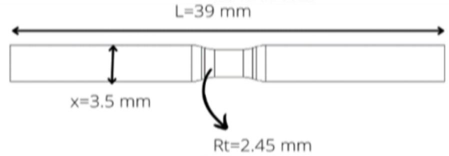
Model C	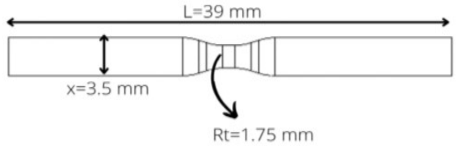
Model D	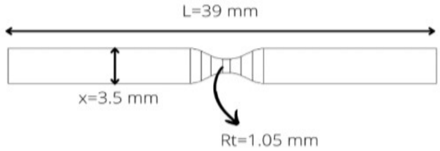

Fig. 2 - Illustration simplified straight of Femoral popliteal artery

2.2 Meshing of femoropopliteal artery model

The simplified FPA model was discretized into meshed region using the Ansys meshing modeller as shown in Figure 3. This model was meshed using the tetrahedron shapes which generated almost 563112 number of nodes and 547808 elements. The proximity and curvature methods were implemented to achieve the sufficient number mesh through the grid independency test (GIT) result. Numerical stability and reliable solutions require a high quality mesh. Mesh generation is also known as grid generation [14]. Grid type and density are determined by the flow domain geometry.

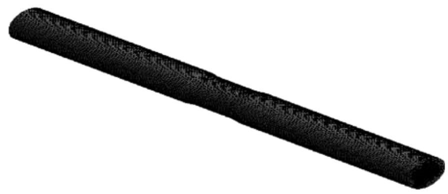

Fig. 3 - The meshing for FPA with stenotic region.

2.3 Parameter assumptions and boundary conditions

In modelling, several flow parameters and properties were considered to be constant. This is due to avoid any complexity of the simulation which might be affected the iteration time. Thus, in this study, blood was assumed as an incompressible flow, Newtonian fluid, and inviscid flow. The blood has a dynamic viscosity of 0.0049kg/ms, and a density of 1060 kg/m^3 [15]. Blood vessels are also assumed to be steady flow and rigid body with the no-slip condition [16]. The computational domain was assigned the boundaries as shown in Figure 4. The proximal inlet was assigned as a velocity whilst the distal end was assigned as a pressure out.

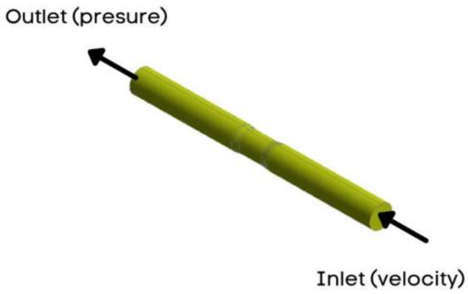

Fig. 4 - Boundary condition of femoropopliteal artery model

Three periodic time phases were imposed in this study; peak systole, mid diastolic and end diastolic times as shown in Table 1.

Table 1 – The periodic velocity values in FPA model

Part	Variable value
Peak Systolic	0.5
End Diastolic	0.05
Mid Diastolic	0.1

2.4 Governing equations

Computational Fluid Dynamics (CFD) method was implemented to analyse and solves issues involving fluid flows using numerical analysis and data structures. Computer software code ANSYS FLUENT 2021 was used as tools simulate free-stream fluid flow and the interaction of fluids with surfaces determined by boundary conditions. CFD has become a helpful technique for predicting detailed information on human blood flows governed by continuity and Navier-Stokes equations. The finite volume method (FDM) was used to solve the fluid flow problems. Detail explanation on the continuity and momentum equation as followed.

Equation (1) is the continuity equation in conservation form,

$$\frac{\delta p}{\delta t} + \nabla.(\rho V) = 0 \quad (1)$$

where t is time, ρ is fluid density, V is the flow velocity vector field. By consider the vector identity, which is defined as the divergence of the product of a scalar and a vector,

$$\nabla.(\rho V) \equiv (\rho \nabla.V) \ (\nabla.\nabla \rho) \quad (2)$$

Substitute Eqn. (1) in the conservation form, Eqn. (2),

$$\frac{\delta p}{\delta t} + (\rho \nabla.V) + (\nabla.\mathrm{V}\rho) = 0 \quad (3)$$

The first two terms on the left side of Eqn. (3) are simply of the substantial derivative of density. As a result, Eqn. (4) becomes,

$$\frac{D\rho}{Dt} + \nabla.(\rho V) = 0 \quad (4)$$

D/Dt = 0 if the fluid is incompressible while ρ is constant. After that, the continuity equation becomes,

$$\nabla.V = 0 \quad (5)$$

The continuous fluid flow through an artery is represented by the Navier-Stokes equations. It is made up of two equations: momentum equation, and continuity equation all of which are determined using fluid flow conservation. The equations can be used as an incompressible Navier-Stokes equation.

$$\rho(\frac{\delta u}{\delta t} + \mu.\nabla \mathrm{u}) = - \nabla \mathrm{P} + \mu \nabla^2 u \quad (6)$$

where V and P represent the blood flow velocity vector and pressure, respectively.

2.5 Hemodynamic effect on the stenoic FPA region

In this study, four different hemodynamic parameters were analyzed; velocity distribution, pressure, WSSlow, and WSS. These parameters had a significant effect to predict the growth of thrombosis, especially in different stenotic FPA models. Detail information on each parameter was explained as followed.

2.5.1 Velocity distribution

The arterial blood flow pattern is described using velocity distribution, which makes the fluid mechanics of the condition flow easier to understand [17]. When the pressure difference, the length and the viscosity are constant, the quantity of flow increases as the radius or velocity increases [18]. In this regard, the results of the simulation of velocity distribution were investigated to understand velocity blood flow in the artery from the artery morphologies.

2.5.2 Pressure

Pressure is one of the hemodynamic parameters that is used to analyse the artery's hemodynamic performance. Numerous studies have investigated pressure's effect on hemodynamic. The vitro study was performed under steady-state conditions, assuming Newtonian flows with 50% stenosis [19]. Kumar and Awasthi also assessed the hemodynamic parameters of pressure and wall shear stress (WSS) in a solid artery to determine the effect of hematocrit percentages. Throughout the study, laminar and Newtonian blood flow was examined in a solid artery with multiple stenoses [20].

2.5.3 Wall Shear Stress

Wall shear stress is one of the factors that contribute to the behaviour of the blood flow in that it causes both thrombosis and atherosclerosis to form [21]. The wall shear stress is caused by friction between the blood and the endothelial layer, which is opposed by circumferential stress and strain in the vessel wall [22]. Several studies have demonstrated that atherosclerosis may be influenced by local hemodynamic conditions, including wall shear stress [23]. The rate of development of atherosclerosis for the WSSlow is less than 4 dyne/cm^2. Thrombosis may occur if the WSS is above 70 dyne/cm^2.

Published by FAZ Publishing
http://www.fazpublishing.com/jcf

3. Results and Discussion

Four types of a femoropopliteal artery with different sizes of stenosis was simulate in three different pulsating times; peak systolic, end diastolic, and mid diastolic times.

3.1 Grid independence test

Grid independence is being tested by changing the sizes of the elements from 1.0 mm to 0.29 mm at the meshing phase to increase the number of nodes from 21658 nodes to 563112 nodes. Figure 5 shows the result of velocity profile femoropopliteal artery models with different number of nodes which are 21658, 128304, 238854, 334425, 444600 and 563112. The selection of node is based on an unchanging result of the parameter with respect to the increasing number of nodes. For this simulation, 444600 nodes with element size of 0.315mm is chosen because of the resulting velocity is almost identical to the 128304, 238854, 334425, and 563112 nodes.

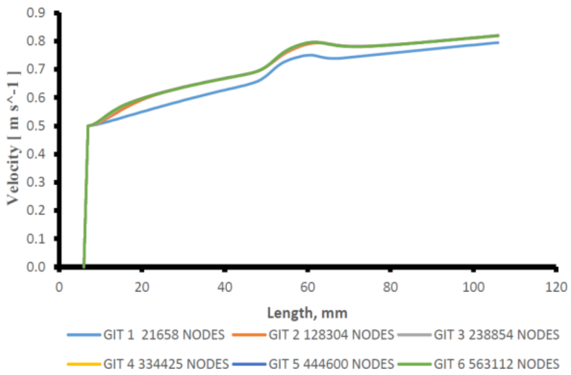

Fig. 5 – Results of six grid independence test

3.2 The effect of velocity at Stenoic Region

Four different stenosis sizes are simulated based on their inlet velocity in the simulation. Those sizes are 0.5 m/s for peak systolic, 0.05 m/s for diastolic, and 0.1 m/s for middle. The graph shown in Figure 6(a) shows the velocity for model A, model B, model C and model D at peak systolic condition. Overall, the velocity distribution throughout these four models is growing. The velocity distribution is almost the same between four models at one point, but velocity distribution increases significantly when velocity enters the stenosis part. The graph shows a sharp increase starting from length 44 mm until the end, with model D with 70% stenosis having the highest velocity distribution. Model A with 10% stenosis has the lowest velocity distribution. When the velocity exits the stenosis part at a length of 60 mm, all four lines show a horizontal pattern.

For mid diastolic, inlet velocity is 0.1 m/s is imposed in simulation. Figure 6(b) shows the velocity of models A, B, C, and D at mid systolic conditions. Based on the observation in Figure 4.6, all fours velocity starts at the same point, which is 0.1 ms^{-1} and grow steadily with almost the same velocity until the velocity reaches the stenosis part at length 40 mm. After the velocity enters the stenosis part, the graph shows all fours line increase drastically and then decreases when velocity out from stenosis area starting from length 60 mm until the end. Model A graph is smoother than other graph's models.

Graph in Figure 6(c) shows the velocity distribution at end diastolic. The four models started at the same point, which is 0.05 ms^{-1} and then went up from length 40 mm to 60 mm, which is a point where stenosis is present in the model. But after out from the stenosis part, velocity distribution becomes decreases. Model D shows a rapid increase followed by a sharp decline. So, when the velocity enters the area of stenosis, it will be faster because the wall of the area of stenosis becomes smaller and narrow. Blood velocity is increase when enter stenosis area but start to decrease when out of stenosis area. The presence of stenosis will increase the velocity. Figure 7(a), 7(b) and 7(c) shows comparison of velocity contour during peak systolic, mid diastolic and end diastolic in four different models.

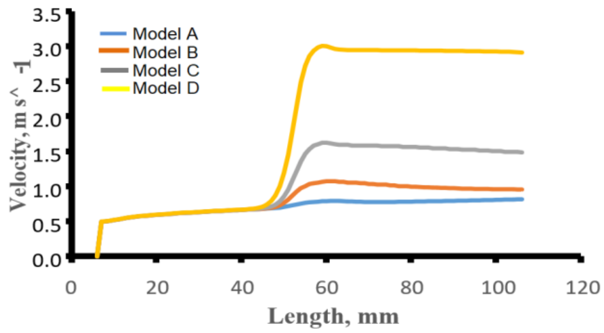

Fig. 6(a) – Velocity distribution along the femoral popliteal artery model for peak systolic

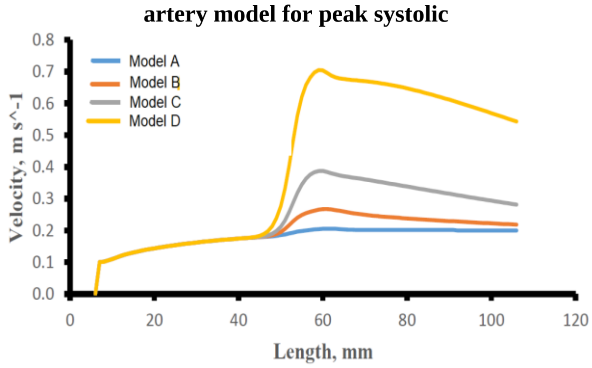

Fig. 6(b) – Velocity distribution along the femoral popliteal artery model for mid diastolic

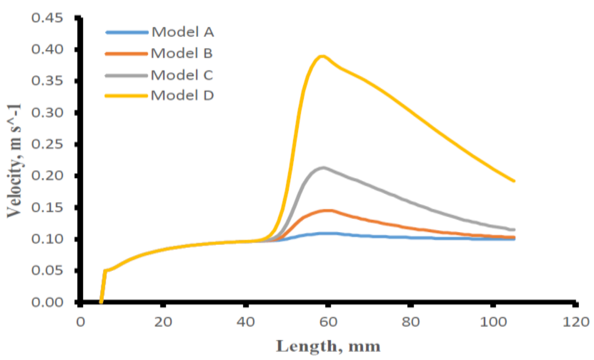

Fig. 6(c) – Velocity along the femoral popliteal artery model for end diastolic

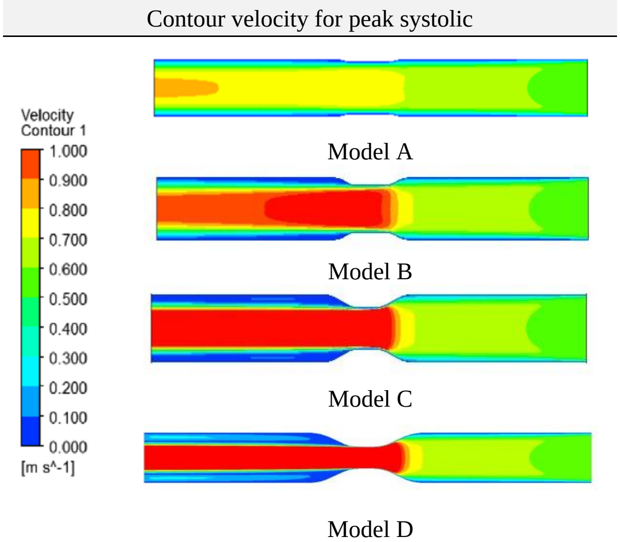

Fig. 7(a) – Velocity contour during peak systolic

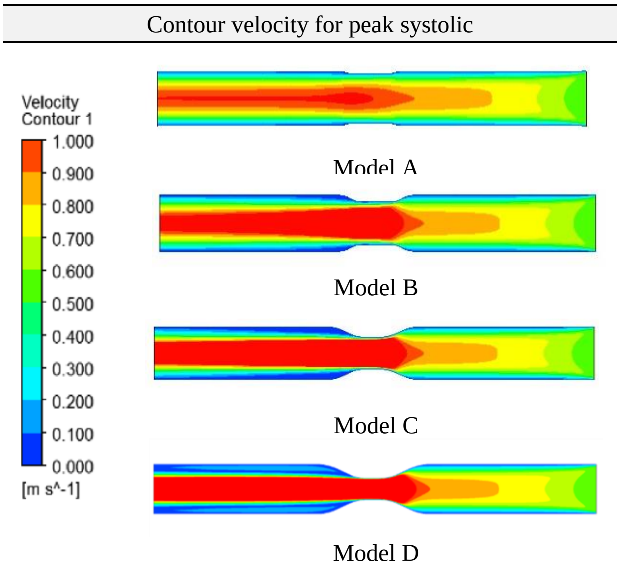

Fig 7(b) – Velocity contour during mid diastolic

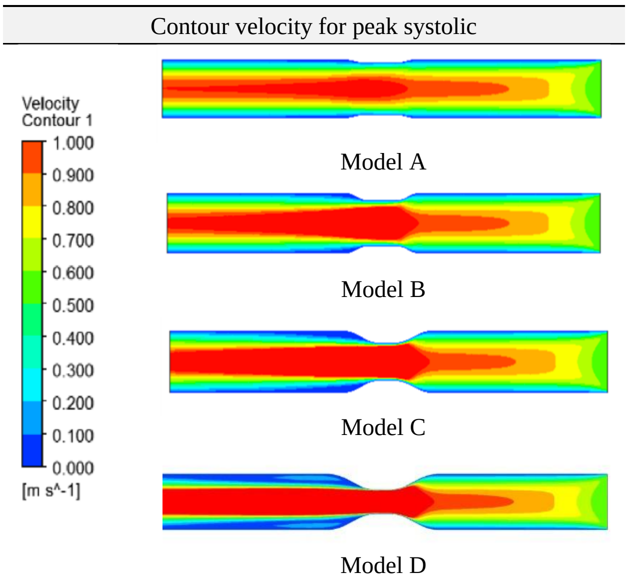

Fig. 7(c) – Velocity contour during end diastolic

3.3 The effect of pressure at Stenoic Region

Stenosis causes pressure drops when the flow increases [24]. During the stenotic period, the pressure graph does not change much, but before leaving the stenotic area, the pressure graph shows a decrease in pressure. In peak conditions, the contour distribution of total pressure is highest for model D, which gives the reading of 4346.24 Pa, then for model C, which comes in at 1067.560 Pa, then for model B, with 385.623 Pa, and finally for model A, with 251.452 Pa. Total pressure at mid diastolic condition shows Model D has the highest total pressure, while model A has the lowest. Model D has the highest starting point, which is 214.838 Pa. As pressure reaches the stenosis area, pressure begins to decrease from point 48 mm to 60 mm. There is a negative value of pressure at the stenosis area at model C and model D. After passing the stenosis area, the pressure value increases slowly. Model D has the most significant impact on total pressure.

At end diastolic time, the pressure decreases steadily from 13.93 Pa to 0 Pa in model A. For model B, the pressure dropped from 16.0217 Pa to 0 Pa, whereas for model C, the pressure dropped from 23.6237 Pa to -4.31777 Pa. Finally, the pressure dropped from 66.5022 Pa to -18.7335 Pa for model D. The model D dramatically dropped in pressure at length 50 mm. This shows the difference in total pressure distribution due to the different size stenosis at the femoropopliteal artery. When the stenosis size increases, the artery will become narrower, resulting in a reduction of arterial pressure. The graph shown in Figure 8(a), 8(b) and 8(c) shows the pressure at three different pulsating times for four models.

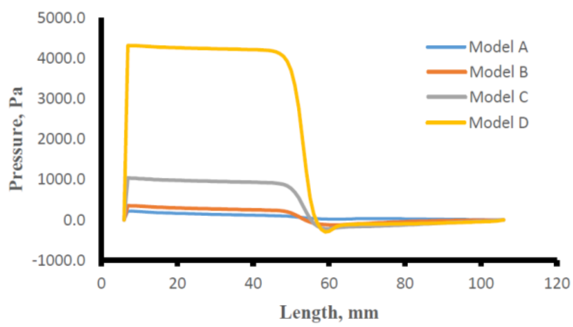

Fig. 8(a) – Total pressure along the femoral popliteal artery model for peak systolic

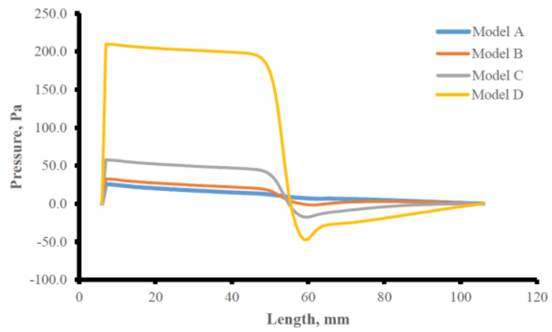

Fig. 8(b) – Total pressure along the femoral popliteal artery model for mid diastolic

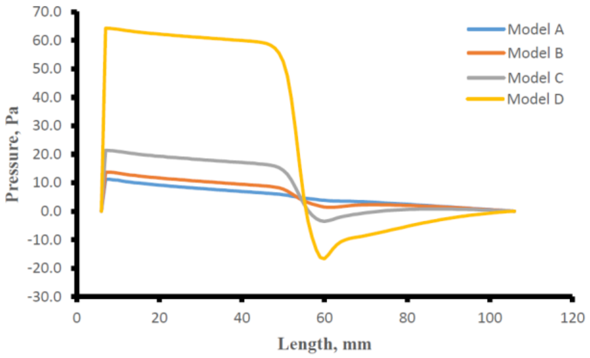

Fig. 8(c) – Velocity distribution along the femoral popliteal artery model for end diastolic

Figure 9(a), 9(b) and 9(c) shows comparison of total pressure during peak systolic, mid diastolic and end diastolic in four different models.

Pressure contour for peak systolic

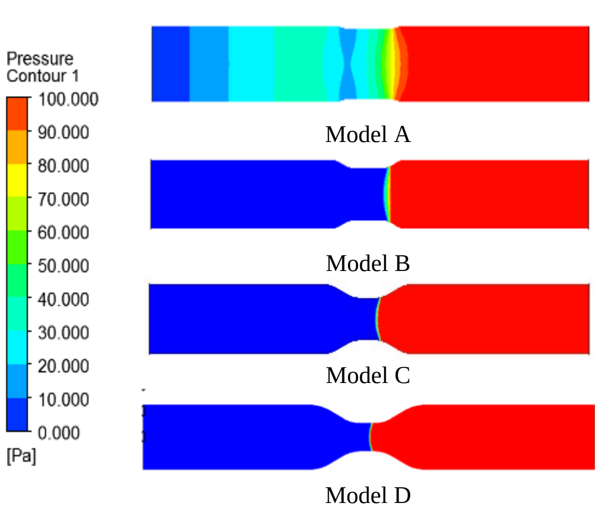

Fig. 9(a) - Comparison of pressure contour total pressure during peak systolic

Pressure contour for peak systolic

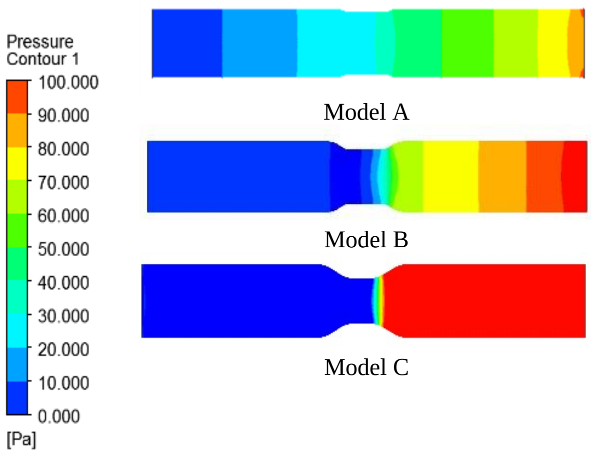

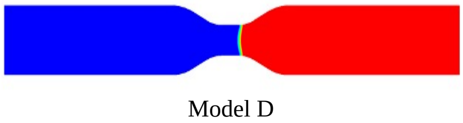

Fig. 9(b) – Comparison of pressure contour total pressure during mid diastolic

Pressure contour for peak systolic

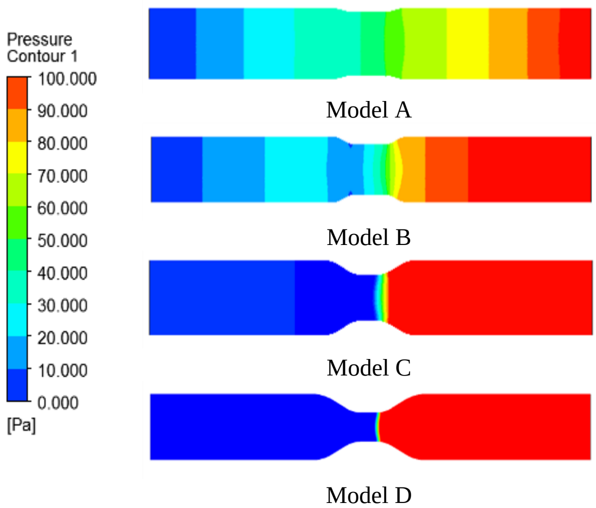

Fig. 9(c) – Comparison of pressure contour total pressure during end diastolic

3.4 Wall Shear Stress (WSS)

The wall shear stress (WSS) plays an important role in the process of atherosclerosis localization, and, low WSSs have been linked to atherosclerosis distribution, and their magnitude has been linked to atherosclerosis severity [25]. The development of atherosclerosis for the WSSlow is predicted to be less than 4 dyne/cm². The prediction for WSS greater than 70 dyne/cm² can lead the formation of thrombosis. A peak systolic condition is represented by an inlet velocity of 0.5 m/s. For femoropopliteal artery models A, B, C, and D, the shear stresses are shown in Figure 10(a) during peak systolic time. Based on the result, model B is the highest tendency for atherosclerosis to occur with area of percentage of 9.3%. In addition, Model B also shows the high prediction of thrombosis with the area of percentage of 13.1% followed by model D and model C with 13% and 12.4%. Model A have the lowest percentage with 6.1%.

The inlet velocity of 0.1 m/s represents mid diastolic condition. Figure 10(b) shows shear stress in the femoropopliteal artery during mid systolic time for models A, B, C, and D. According to the results, model C has the greatest tendency for atherosclerosis to develop with 46.9% followed by model B and model D with 43.8% and 16.3%. Model A has the lowest percentage of atherosclerosis with 8.4%. Model A, model B, and model C show no signs of thrombosis. However, model D shows the presence of thrombosis with the area of percentage of 4%. For end diastolic condition, inlet velocity is 0.05 ms^{-1} is imposed in simulation. Figure 10(c) shows the shear stress that occur at femoropopliteal artery model A, B, C and D in end diastolic condition. At end diastolic time, the highest percentage of WSS*low* is 95.9% for model A. Model B, model C and model D have similar percentage value with 88.3% for model C and 87.9 for both model B and model D. The results indicate that all four models have high rates of atherosclerosis development at diastolic time.

Wall shear stress contour for peak systolic

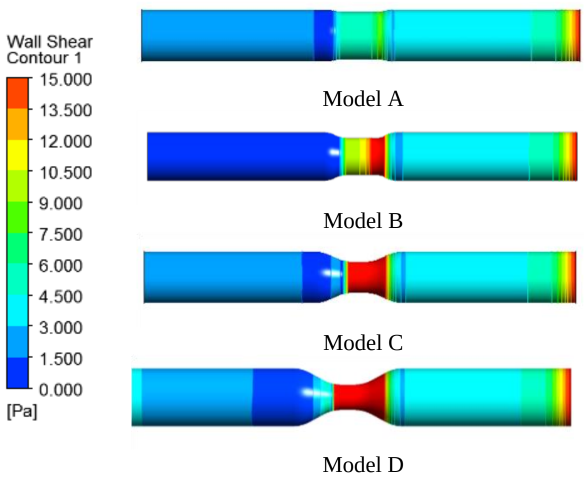

Figure 10(a): Contour of wall shear stress at femoropopliteal artery in peak diastolic condition

Wall shear stress contour for peak systolic

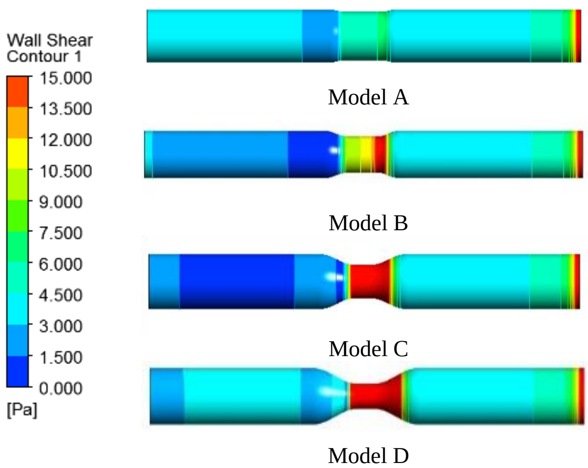

Figure 10(b): Contour of wall shear stress at femoropopliteal artery in mid diastolic condition

Wall shear stress contour for peak systolic

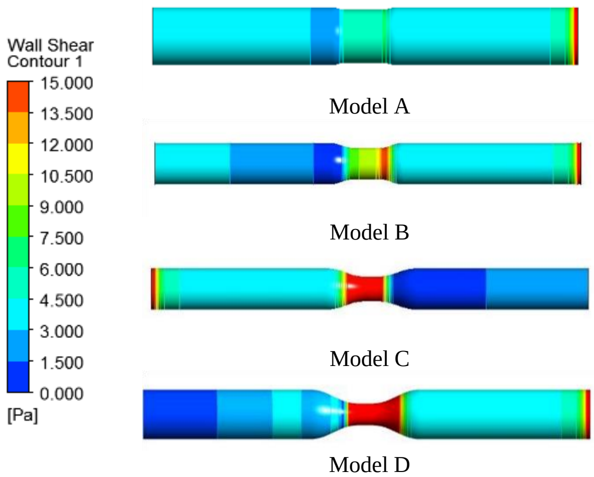

Figure 10(c): Contour of wall shear stress at femoropopliteal artery in end diastolic condition

3.5 Verification with previous study

Verification is the process of comparing the results of computations with known solutions [26]. Comparing simulation results with previous study results is an effort to demonstrate how accurate a CFD simulation can be so that they may be used with confidence for this simulation and the results can be considered credible to do any analysis. In this study, only one case was selected which is cases with 50% stenosis and from three different pulsating time, peak systolic condition was chosen. Based on study by [27], one model has been created. This model geometry is based on the previous study as shown in Figure 11 and 12 shows a model that has been created for the verification process.

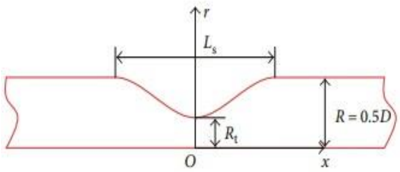

Fig. 11 – Axis symmetrical tube model of the stenosis artery from previous study

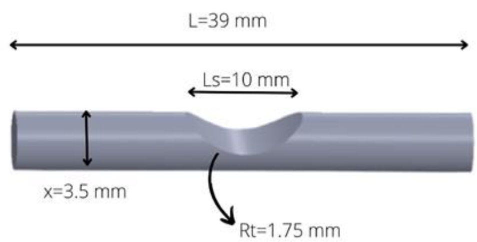

Fig. 12 – Model of the stenosis artery based on geometry from previous study

Pressure data and z-axis data was taken and compared with pressure data and x-axis data from 50% stenosis case at peak systolic condition. Because the axis is different, to make data comparable, the dimensionless graph is created by dividing all data from the x-axis simulation and z-axis model previous study with the highest value on their y-axis. Pressure data from both simulations were also divided with the highest data from their x-axis data. Figure 12 shows dimensionless graph for 50% stenosis at peak systolic condition.

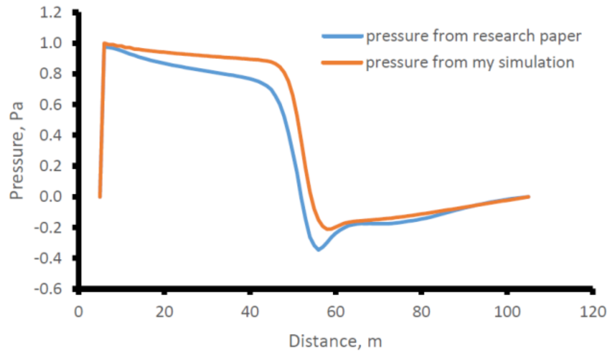

Fig. 13 – Dimensional graph for 50% stenosis at peak systolic condition for both simulations

4. Conclusion

Therefore, it can be concluded that variations in the size of stenoses affected hemodynamic factors in blood. As stenosis develops, the velocity will increase, but pressure will decrease. In addition, this study successfully achieved its objective of investigating the flow characteristics for different sizes of stenosis at the femoropopliteal artery

Acknowledgement

The support of the Ministry of Education under the FRGS/1/2018/TK03/UTHM/03/ and the Universiti Tun Hussein Onn Malaysia (UTHM) grant number K058, the Faculty of Mechanical and Manufacturing Engineering and Flow Analysis, Simulation and Turbulence Research Group (FASTREG) for its support.

References

[1] W. S. Aronow, "Peripheral arterial disease of the lower extremities," (2012): doi: 10.5114/aoms.2012.28568.

[2] D. S. Sankar, "Pulsatile flow of a two-fluid model for blood flow through arterial stenosis," *Math. Probl. Eng.*, vol. 2010, (2010): doi: 10.1155/2010/465835.

[3] S. Sriyab,"Mathematical analysis of non-Newtonian blood flow in stenosis narrow arteries," *Comput. Math. Methods Med.*, vol. 2014, (2014): doi: 10.1155/2014/479152.

[4] S. Sandeep and S. R. Shine, "Effect of stenosis and dilatation on the hemodynamic parameters associated with left coronary artery," *Comput. Methods Programs Biomed.*, vol. 204, p. 106052, (Jun 2021): doi: 10.1016/j.cmpb.2021.106052.

[5] D. F. Young and F. Y. Tsai, "Flow characteristics in models of arterial stenoses - I. Steady flow," *J. Biomech.*, vol. 6, no. 4, pp. 395–410, (Jul. 1973): doi: 10.1016/0021-9290(73)90099-7.

[6] D. Perloff, C. Grim, J. Flack, and E. D. Frohlich, "AHA Medical / Scientific Statement Human Blood Pressure Determination by Sphygmomanometry," *Library (Lond).*, (2012): pp. 2460–2470.

[7] M. Brust *et al.*, "Rheology of human blood plasma: Viscoelastic versus Newtonian behavior," *Phys. Rev. Lett.*, vol. 110, no. 7, (2013): doi: 10.1103/PhysRevLett.110.078305.

[8] J. M. C. Yunus A. Cengel, "Fluid Mechanics: Fundimental and Application," *Вестник Казнму*, vol 3, (2013): p. c.30.

[9] X. He and D. N. Ku, (1996) "Pulsatile flow in the human left coronary artery bifurcation: Average conditions," *J. Biomech. Eng.*, vol. 118, no. 1, (1996): pp. 74–82, doi: 10.1115/1.2795948.

[10] J. Rosser and D. J. Thomas, Bioreactor *processes for maturation of 3D bioprinted tissue*. Elsevier Ltd. (2018):

[11] A. M. Shaaban and A. J. Duerinckx, "Wall shear stress and early atherosclerosis: A review," *Am. J. Roentgenol.*, vol. 174, no. 6, (2000) pp. 1657–1665, doi: 10.2214/ajr.174.6.1741657.

[12] J. Murphy and F. Boyle, "Predicting neointimal hyperplasia in stented arteries using timedependant computational fluid dynamics: A review," *Comput. Biol. Med.*, vol. 40, no. 4, (2010): pp. 408–418, doi: 10.1016/j.compbiomed.2010.02.005.

[13] M. S. A. Paisal *et al.*, "C," in *IOP Conference Series: Materials Science and Engineering*, vol. 226, no. 1, (2017): doi: 10.1088/1757-899X/226/1/012147.

[14] A. Lintermann, *Computational Meshing for CFD Simulations.* (2012)

[15] A. Kaha *et al.*, "Lumped parameter modelling in femoral popliteal artery for normal and severe conditions," *Int. J. Integr. Eng.*, vol. 10, no. 5, (2018): pp. 193–203, doi: 10.30880/ijie.2018.10.05.029.

[16] Y. Jiang, J. Zhang, and W. Zhao, "Effects of the inlet conditions and blood models on accurate prediction of hemodynamics in the stented coronary arteries," *AIP Adv.*, vol. 5, no. 5, (2015): doi: 10.1063/1.4919937.

[17] E. Science, "Velocity distribution in aortic flow',". (1973):

[18] O. A. Olowoyeye, S. E. G. Chiu, G. Leung, G. A. Wright, and A. R. Moody, "Analysis of the Velocity Profile of the Popliteal Artery and Its Relevance During Blood Flow Studies," (2017): doi: 10.1177/8756479317716394.

[19] M. Jahangiri, M. Saghafian, and M. R. Sadeghi, "Numerical simulation of hemodynamic parameters of turbulent and pulsatile blood flow in flexible artery with single and double stenoses Numerical simulation of hemodynamic parameters of turbulent and pulsatile blood flow in flexible artery with single and double stenoses †," no. March, (2015): pp. 15–18, doi: 10.1007/s12206-015-0752-3.

[20] S. R. Shah, S. U. Siddiqui, and A. Singh, "Mathematical Modeling and Numerical Simulation of Blood Flow through Tapered Artery," vol. 3, no. 2, (2016): pp. 710–717.

[21] S. Nilsson and L. Bergstrand, "TECHNICAL NOTE," vol. 29, no. 4, (1996): pp. 543–547.

[22] D. Lu and G. S. Kassab, "Role of shear stress and stretch in vascular mechanobiology," no. July, (2011): pp. 1379–1385.

[23] Markl *et al.*, "In Vivo Wall Shear Stress Distribution in the Carotid Artery Effect of (2010): Bifurcation Geometry, Internal Carotid Artery Stenosis" pp. 647–655, doi: 10.1161/CIRCIMAGING.110.958504.

[24] D. F. Young, N. R. Cholvin, R. L. Kirkeeide, and A. C. Roth, "Hemodynamics of arterial stenoses at elevated flow

rates," *Circ. Res.*, vol. 41, no. 1, (1997): pp. 99–107, doi: 10.1161/01.RES.41.1.99.

[25] A. Buradi and A. Mahalingam, "Effect of stenosis severity on wall shear stress based hemodynamic descriptors using multiphase mixture theory," *J. Appl. Fluid Mech.*, vol. 11, no. 6, (2018): pp. 1497–1509, doi: 10.29252/jafm.11.06.29062.

[26] C. J. Roy and W. L. Oberkampf, "Verification and validation in computational fluid dynamics," *Handb. Fluid Dyn. Second Ed.*, no. March, (2016): pp. 44.1-44.11, doi: 10.1201/b19031-50.

[27] Y. Zhou, C. Lee, and J. Wang, "The computational fluid dynamics analyses on hemodynamic characteristics in stenosed arterial models," *J. Healthc. Eng.*, vol. 2018, (2018): doi: 10.1155/2018/4312415.